TEST OF OPTICAL STOCHASTIC COOLING IN FERMILAB*

V. A. Lebedev#, FNAL, Batavia, IL 60510, USA
M. S. Zolotorev, LBNL, Berkeley, CA 94720, USA

Abstract

A new 150 MeV electron storage ring is planned to be build at Fermilab. The construction of a new machine pursues two goals a test of highly non-linear integrable optics and a test of optical stochastic cooling (OSC). This paper discusses details of OSC arrangements and choice of major parameters of the cooling scheme. At the first step the cooling will be achieved without optical amplifier (OA). It should introduce the damping rates higher than the cooling rates due to synchrotron radiation. At the second step we plan to use an OA. The passive cooling scheme looks as a promising technique for the LHC luminosity upgrade. Its details are also discussed.

INTRODUCTION

The stochastic cooling suggested by Simon Van der Meer [1,2] has been successfully used in a number of machines for particle cooling and accumulation. However it is not helpful for cooling of dense bunched beams in proton-(anti)proton colliders. In the case of optimal cooling the maximum damping rate can be estimated as:

$$1/\tau \approx 2W\sigma_s/(NC) \ ,$$

where W is the bandwidth of the system, N is the number of particles in the bunch, σ_s is the rms bunch length, and C is the machine circumference. For the LHC proton beam (σ_s = 9 cm, C = 26.66 km) and one octave system band with upper boundary of 8 GHz one obtains τ = 12000 hour. Effective cooling requires damping rates that are higher by at least 3 orders of magnitude. The OSC suggested in Ref. [3] can have a bandwidth of ~10^{14} Hz and, thus, suggests a way to achieve required damping rates. The basic principles of the OSC are similar to the normal (microwave) stochastic cooling. The key difference is the use of optical frequencies, which allow an increase of system bandwidth by 4 orders of magnitude.

In the OSC a particle emits e.-m. radiation in the first (pickup) wiggler. Then, the radiation amplified in an OA makes a longitudinal kick to the particle in the second (kicker) wiggler as shown in Figure 1. Further we will call these wigglers as the pickup and the kicker. A magnetic chicane is used to make space for an OA and to bring the particle and the radiation together in the kicker wiggler. In further consideration we assume that the path lengths of particle and radiation are adjusted so that the relative particle momentum change is equal to:

$$\delta p/p = -\kappa \sin(k\,\Delta s) \ . \qquad (1)$$

Here $k = 2\pi/\lambda$ is the radiation wave number, and Δs is the particle displacement on the way from pickup to kicker relative to the reference particle which obtains zero kick:

$$\Delta s = M_{51}x + M_{52}\theta_x + M_{56}(\Delta p/p) \ . \qquad (2)$$

Here M_{5n} are the elements of 6x6 transfer matrix from pickup to kicker, x, θ_x and $\Delta p/p$ are the particle coordinate, angle and relative momentum deviation in the pickup center.

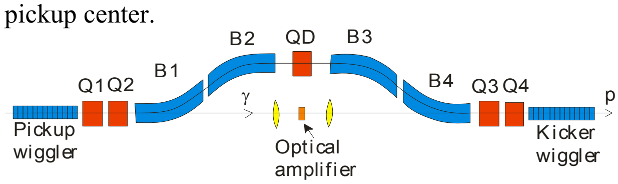

Figure 1: OSC schematic.

For small amplitude oscillations the horizontal and vertical cooling rates are [4]:

$$\begin{bmatrix}\lambda_x\\ \lambda_s\end{bmatrix} = \frac{k\kappa}{2}\begin{bmatrix}M_{56} - C\eta_{pk}\\ C\eta_{pk}\end{bmatrix} \ , \qquad (3)$$

where $\eta_{pk} = (M_{51}D_p + M_{52}D'_p + M_{56})/C$ is the partial momentum compaction determined so that for a particle without betatron oscillations and with momentum deviation $\Delta p/p$ the longitudinal displacement relative to the reference particle on the way from pickup to kicker is equal to $C\eta_{pk}\,\Delta p/p$, and D and D' are the dispersion and its derivative. Here we also assume that there is no x-y coupling. Introduction of x-y coupling outside the cooling area allows redistribution of the horizontal damping rate into both transverse planes. The sum of damping rates, $\Sigma\lambda_n = k\kappa M_{56}/2$, does not depend on the beam optics outside of the cooling chicane.

An increase of betatron and synchrotron amplitudes results in a decrease of damping rates [4]:

$$\begin{aligned}\lambda_x(a_x,a_s) &= F_x(a_x,a_s)\lambda_x \ ,\\ \lambda_s(a_x,a_s) &= F_s(a_x,a_s)\lambda_s \ ,\end{aligned} \qquad (4)$$

where the fudge factors are:

$$\begin{aligned}F_x(a_x,a_s) &= 2J_0(a_s)J_1(a_x)/a_x \ ,\\ F_s(a_x,a_s) &= 2J_0(a_x)J_1(a_s)/a_s \ ,\end{aligned} \qquad (5)$$

and a_x and a_s are the amplitudes of longitudinal particle motion due to betatron and synchrotron oscillations expressed in the units of e.-m. wave phase:

$$\begin{aligned}a_x &= k\sqrt{\varepsilon_1\left(\beta_p M_{51}{}^2 - 2\alpha_p M_{51}M_{52} + \left(1+\alpha_p{}^2\right)M_{52}{}^2\right)} \ ,\\ a_p &= kC\left|\eta_{pk}\right|(\Delta p/p)_{\max} \ .\end{aligned} \qquad (6)$$

Here ε_1 is the Courant-Snyder invariant of a particle, and $(\Delta p/p)_{\max}$ is the particle maximum momentum deviation. As one can see from Eqs. (4) and (5) a damping rate changes its sign if any of amplitudes exceeds the first root of the Bessel function $J_0(x)$, $a_{x,}a_s > \mu_0 \approx 2.405$.

The following conclusions can be drawn from Eqs. (3) and (6). M_{56} depends only on focusing inside the chicane, while η_{pk} additionally depends on the dispersion at the

*Work supported by Fermi Research Alliance, LLC, under Contract No. DE-AC02-07CH11359 with the United States Dep. of Energy
#val@fnal.gov

ISBN 978-3-95450-118-2

chicane beginning, *i.e.* on the optics in the rest of the ring. Consequently, the ratio of damping rates,

$$\lambda_x / \lambda_s = M_{56} / C\eta_{pk} - 1 \ , \tag{7}$$

and the longitudinal cooling range,

$$n_{\sigma s} \equiv (\Delta p / p)_{max} / \sigma_p = \mu_0 / |kC\eta_{pk}\sigma_p| \ , \tag{8}$$

depend on focusing and dispersion inside the chicane, but do not depend on behaviour of the beta-function. Here σ_p is the relative rms momentum spread. On contrary, the transverse cooling range,

$$n_{\sigma x} \equiv \frac{\varepsilon_{\max}}{\varepsilon} = \frac{\mu_0^2 / \left(k^2 \varepsilon\right)}{\beta_p M_{51}^2 - 2\alpha_p M_{51} M_{52} + \left(1+\alpha_p^2\right) M_{52}^2} \ , \tag{9}$$

does not depend on the dispersion behaviour but depends on the beta-function behaviour. Here ε is the rms momentum spread.

Below we consider two cooling schemes. The first one is passive where radiation is focused into the kicker wiggler but is not amplified; and the second one is active where an OA is used. Both of them have their advantages and drawbacks. In the case of passive cooling one does not need an amplifier and, consequently, can use higher optical frequencies and larger bandwidth which boost the gain. It also requires smaller path difference which considerably increases the cooling ranges, $n_{\sigma s}$ and $n_{\sigma x}$. In the case of active system one can reduce the length and magnetic field of the wigglers, but it requires an additional delay in the chicane to compensate a delay in the OA (~5 mm). Making an amplifier at required power and wavelength can be a challenging problem too.

Table 1: Main Parameters of IOTA Storage Ring

Circumference	38.7 m
Nominal beam energy	150 MeV
Bending field	7.2 kG
Betatron tune	3.5 ÷ 7.2
Maximum β-function	3 ÷ 9 m
Transverse emittance, rms	3 nm
Rms momentum spread, σ_p	$1.5 \cdot 10^{-4}$
SR damping rates (ampl.), $\lambda_s / \lambda_\perp$	4 / 2 s^{-1}

BEAM OPTICS

The main parameters of the ring, called IOTA [5], are shown in the Table 1. The OSC system will take one of four straight sections with length of ~5 m. The beta-function and dispersion in the section are presented in Figure 2. The optics was optimized for 800 nm radiation where an optical amplifier is feasible. The following limitations were taken into account in the optics design. The chicane should separate the radiation and the beam by 40 mm making a sufficiently large separation between the electron beam and the OA. The cooling ranges before the OSC is engaged, $n_{\sigma s}$ and $n_{\sigma x}$, have to be large enough so that the major fraction of the beam would be cooled. The path length difference acquired by electron beam in the chicane has to be sufficiently large to compensate delay in OA. Note that the rectangular dipoles do not produce horizontal focusing. Therefore in the absence of other focusing inside the chicane the partial slip factor is equal to M_{56}/C and does not depend on the dispersion. Consequently, there is no transverse cooling. To achieve transverse cooling a defocusing quad was introduced in the chicane center. The strength of this quad is limited by reduction of transverse cooling range, $n_{\sigma x}$. That required sufficiently large dispersion in the chicane. The major parameters of the cooling section are presented in Table 2.

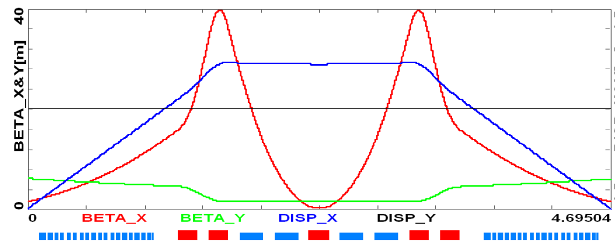

Figure 2: Optics functions in the OSC section.

Table 2: Major Parameters of Chicane Beam Optics

M_{56}	8.7 mm
Cooling rates ratio, λ_x/λ_s	7.5
Horizontal beam separation	40 mm
Delay in the chicane	4.5 mm
Cooling ranges (before OSC), $n_{\sigma x}/n_{\sigma s}$	3.5 / 2
Dipole magnetic field	4 kG
Dipole length	18 cm
Strength of central quad, *GdL*	1.52 kG

The rms emittance and momentum spread are comparatively large for the chosen wavelength of 800 nm. To accommodate it the optics was tuned to maximize the cooling ranges. In particular, we choose (1) the large cooling rates ratio to increase $n_{\sigma s}$, and (2) small beta-function in the chicane center (2 cm) to increase $n_{\sigma x}$. That resulted in high sensitivity to cooling parameters. Simulations show that relative accuracies should be of ~1% for the horizontal beta-function, ~2 cm for the dispersion, and ~2% for the focusing strength of central quadrupole (see Figure 3).

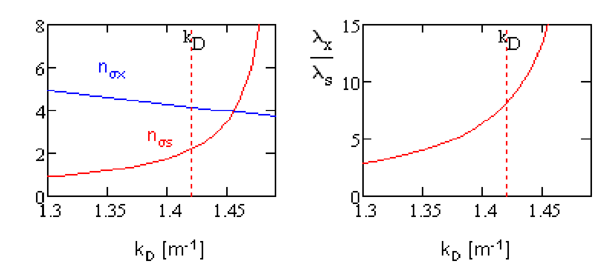

Figure 3: Dependencies of cooling ranges (left) and ratio of damping rates on focusing strength of central quad.

LIGHT OPTICS

Let the coordinates of a particle moving in a flat undulator to depend on time as following:

$$\mathrm{v}_x = c\theta_e \sin\tau' \ , \qquad \mathrm{v}_y = 0 \ ,$$
$$\mathrm{v}_z = c\left(1 - \frac{1}{2\gamma^2} - \frac{\theta_e^2}{2}\sin^2\tau'\right) , \qquad \tau' = \omega_u t' + \psi \ , \tag{10}$$

ISBN 978-3-95450-118-2

where γ is the particle relativistic factor ($\gamma >> 1$), and ω_u is the frequency of particle motion in the undulator.. Substituting velocities of Eq. (10) to the Liénard-Wiechert formula [6] for the horizontal component of electric field in the far zone one obtains:

$$E_x(r,t) = 4e\omega_u\gamma^4\theta_e\cos\tau' \times \frac{1+\gamma^2\left(\theta^2\left(1-2\cos^2\phi\right)-2\theta\theta_e\sin\tau'\cos\phi-\theta_e^2\sin^2\tau'\right)}{cR\left(1+\gamma^2\left(\theta^2+2\theta\theta_e\sin\tau'\cos\phi+\theta_e^2\sin^2\tau'\right)\right)^3}, \quad (11)$$

where θ and ϕ are the angles in the polar coordinate system for the vector from the radiation point, $\mathbf{r}'$, to the observation point, $\mathbf{r}$, $R = |\mathbf{r} - \mathbf{r}'|$, and $t - t' = R/c$. In further calculations we only keep the first harmonic of radiation,

$$E_\omega(r) = \frac{\omega(\theta)}{\pi}\int_0^{2\pi/\omega(\theta)} E_x(r,t)\,\mathrm{e}^{-i\omega t}\,dt, \quad , \quad (12)$$
$$\omega(\theta) = 2\gamma^2\omega_u / \left(1+\gamma^2\left(\theta^2+\theta_e^2/2\right)\right),$$

assuming that the radiation of higher harmonics is absorbed in the lenses and not amplified by OA (if present). Then, applying the Kirchhoff formula to the electric field of Eq. (12),

$$E(r'') = \frac{1}{2\pi i c}\int_S \frac{\omega(\theta)E_\omega(r)}{|r''-r|}\mathrm{e}^{i\omega(\theta)|r''-r|/c}\,ds, \quad (13)$$

one obtains the electric field in the focal point. Accounting a delay in the lens reduces the exponent in Eq. (13) to a complex constant omitted below. For large acceptance lens, $\theta_m \geq \theta_e + 3/\gamma$, located in the middle of the pickup-to-kicker distance the results of numerical integration can be interpolated by the following equation:

$$E_x = 4e\omega_u^2\gamma^4\theta_e F(\gamma\theta_e)/(3c^2), \quad (14)$$
$$F(K) \approx 1/\left(1+1.07K^2+.11K^2+.36K^4\right), 0 \leq K \leq 4,$$

where $K = \gamma\theta_e$ is the undulator parameter, and θ_m is the lens angular size from the radiation point. Integrating the force along the kicker length one obtains the longitudinal kick amplitude in a flat undulator:

$$c\delta p_{\max} = 2\pi\alpha_F m\hbar\omega_0 K^2\left(1+K^2/2\right)F(K)F_u(\kappa_u)/3, \quad (15)$$
$$F_u(\kappa_u) = \mathrm{J}_0(\kappa_u) - \mathrm{J}_1(\kappa_u), \quad \kappa_u = K^2/\left(4\left(1+K^2/2\right)\right).$$

Here m is the number of undulator periods, $\alpha_F = e^2/\hbar c$ is the fine structure constant, $\omega_0 = \omega(0)$, and $c\delta p_{max} \equiv \kappa cp$.

Above we assumed that the radiation emitted by a particle in the course of its motion in the pickup is focused to the location of the same particle in the kicker (when the particle arrives to it) in the course of particle entire motion in the kicker. It is achieved for the lens located at the infinity (*i.e.* if the distance to the lens is much larger than the length of wiggler) – the condition which is impossible to achieve in practice. A practical solution can be obtained with lens telescope which has the transfer matrix $\mathbf{M}_T$ from the center of pickup to the center of kicker equal to $\pm\mathbf{I}$, where $\mathbf{I}$ is the identity matrix. In this case the transfer matrix between emitting and receiving points is $\mathbf{O}(l)\mathbf{M}_T\,\mathbf{O}(-l) = \pm\mathbf{I}$, where $\mathbf{O}(l)$ is the transfer matrix of a drift with length l. The simplest telescope has 3 lenses as shown in Figure 4. For symmetrically located lenses their focusing distances are:

$$F_1 = \frac{LL_1}{L+L_1}, \quad F_2 = \frac{L_1^2}{2(L+L_1)} \quad . \quad (16)$$

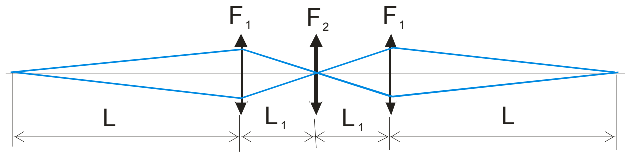

Figure 4: Light optics layout for passive cooling.

Table 3 presents main parameters of undulators, light optics and OSC damping rates for passive and active OSC. The passive OSC requires about one octave band (0.8-1.6 μm). The wave packet lengthening looks satisfactory for 4.5 mm light delay in MgF_2. However a suppression of transverse focusing chromaticity looks as an extremely challenging problem and needs a study. A combination of glasses with normal and abnormal dispersions looks as a good direction to start. A Ti:sapphire OA is considered as a good candidate capable to deliver ~20 Db gain within the allocated signal delay. Conceptual design is progressing.

Table 3: Main Parameters of OSC

Undulator parameter, K	1.5
Undulator period, $2\pi c/\omega_u$	6.53 cm
Number of periods, m	14
Total undulator length, L_w	0.915 m
Distance between undulators	3.6 m
Telescope length, $2L_1$	0.25 m
Telescope aperture, $2a$	40 mm
Lens focal distances, F_1 / F_2	116 / 4.3 mm
Damping rates of passive OSC($x/y/s$)	100/100/25 s^{-1}
Damp. rates 20 Db gain & 10% band	300/300/75 s^{-1}

DISCUSSION

OSC in the LHC looks as a good candidate for the luminosity levelling. Small LHC momentum spread and emittance allow usage of quite short wave lengths, ~300 nm. In this case a passive OSC may be a possible. However handling chromaticity of light optics looks challenging and requires an experimental study. A demonstration of OSC at IOTA should clarify its possible application to the LHC.

REFERENCES

[1] S. Van der Meer, "Stochastic damping of betatron oscillations", internal report CERN/ISR PO/72/31 (1972).
[2] J. Bisognano and C. Leemann, "Stochastic Cooling" in 1981 Summer School on High En. Part. Accelerators, AIP Conf. Proceedings 87, Melville, NY, 1982, pp. 584-655.
[3] M. S. Zolotorev and A. A Zholents, Phys. Rev. E, **50**, 4, p. 3087 (1994).
[4] V. Lebedev, p. 644, HB-2010, (2012).
[5] S. Nagaitsev, *et. al.*, p.16, IPAC-2012, (2012).
[6] L. D. Landau, "Classical theory of fields", Nauka (1973).

ISBN 978-3-95450-118-2